



Microlensing of Kepler Stars as a Method of Detecting Primordial Black Hole Dark Matter

Kim Griest,¹ Matthew J. Lehner,^{2,3} Agnieszka M. Cieplak,¹ and Bhuvnesh Jain³

¹*Department of Physics, University of California, San Diego, California 92093, USA*

²*Institute of Astronomy and Astrophysics, Academia Sinica, P.O. Box 23-141, Taipei 106, Taiwan*

³*Department of Physics and Astronomy, University of Pennsylvania, Philadelphia, Pennsylvania 19104, USA*

(Received 11 August 2011; revised manuscript received 29 September 2011; published 1 December 2011)

If the dark matter consists of primordial black holes (PBHs), we show that gravitational lensing of stars being monitored by NASA's Kepler search for extrasolar planets can cause significant numbers of detectable microlensing events. A search through the roughly 150 000 light curves would result in large numbers of detectable events for PBHs in the mass range $5 \times 10^{-10} M_{\odot}$ to $10^{-4} M_{\odot}$. Nondetection of these events would close almost 2 orders of magnitude of the mass window for PBH dark matter. The microlensing rate is higher than previously noticed due to a combination of the exceptional photometric precision of the Kepler mission and the increase in cross section due to the large angular sizes of the relatively nearby Kepler field stars. We also present a new formalism for calculating optical depth and microlensing rates in the presence of large finite-source effects.

DOI: 10.1103/PhysRevLett.107.231101

PACS numbers: 98.62.Sb, 95.35.+d, 97.60.Lf, 98.35.Jk

Introduction.—Primordial black holes (PBHs) have been considered as a candidate for dark matter (DM) since the days of Hawking [1,2] and PBHs are recently reemerging as objects of intense study [3–5]. PBHs can form from density perturbations at nearly any time during the early Universe with masses typically peaked near the mass enclosed in the particle horizon at that epoch. There have been many ideas on how such perturbations could result, for example, from specific types of inflation, phase transitions in the Early Universe, bubble collisions, domain walls, string loop collapse, etc. See, for example, Refs. [3,5,6] for reviews and many references. If PBHs form early enough they can evade the big bang nucleosynthesis limits on baryons, satisfy Cosmic Microwave Background constraints, and make up the entirety of the dark matter.

Given the large number of theoretical ideas for their formation, there is currently no one compelling mass range for PBH DM. However, there has been extensive experimental and theoretical work that has eliminated most mass ranges, starting with $m_{\text{PBH}} > 10^{-18} M_{\odot}$ [1,2] for PBHs to not have evaporated by today. Currently most mass ranges from $10^{-18} M_{\odot}$ to $10^{16} M_{\odot}$ are ruled out, with the exception being the 5 orders of magnitude between $10^{-13} M_{\odot} < m_{\text{PBH}} < 10^{-7} M_{\odot}$, which we call the PBH DM window. See Refs. [3,4] for recent summaries of these constraints.

As we show below, microlensing of Kepler source stars can detect or rule out PBH DM over a large fraction of the PBH DM window. Thus, if the DM consists of PBHs, the experiment we propose here has an excellent chance of detecting it. Since gravitational microlensing is sensitive to any massive compact halo object (MACHO) a detection or limit would actually be more general than just PBH DM.

The NASA Kepler satellite is a 1 m aperture telescope with a 115 deg^2 field-of-view in an Earth trailing heliocentric orbit, which is currently taking photometric

measurements of around 150 000 stars every 30 minutes [7–9]. The telescope was launched in March 2009 and will point at the same field (in the Cygnus-Lyra region of the sky) for at least 3.5 years. The goal of the Kepler mission is to find extra-solar planets via small decreases in stellar flux due to rare planetary transits in front of the host star in edge-on systems. Very precise photometry is required to detect the tiny decrease in flux that an Earth size planet causes during a transit.

While much of the data are still proprietary, in what follows we analyze a small portion of it to investigate its potential use in a microlensing experiment [10]. Looking through a portion of this publicly available data we see that Kepler source stars have V magnitudes between roughly 10 and 16, have distances from the Earth between 0.9 and 3 kpc, have stellar radii, R_* , between $0.9 R_{\odot}$ and $1.5 R_{\odot}$ (for main sequence stars), or $5 R_{\odot} < R_* < 20 R_{\odot}$ (for giant stars) and have photometric errors per observation between 20 and 1000 ppm (with most between 300 and 1000 pm).

Microlensing and analytic estimate.—Microlensing searches for low mass objects have been performed and have returned significant limits on any massive compact halo objects, including PBHs, that might constitute the dark matter [11–14].

These microlensing surveys examined tens of millions of stars in the Large Magellanic Cloud (LMC), which is at a distance of 50 kpc, for periods of many years. Since the naive microlensing optical depth increases with source star distance and the total microlensing event rate is proportional to the number of monitored stars times the duration of the survey, it might be surprising that the many fewer Kepler light curves on much closer stars, can provide stronger limits on low mass DM in certain mass ranges than these surveys have.

As calculated below, this is due to several factors. First, the extreme precision of the Kepler photometry allows very small magnifications to be detected. Requiring a sequence of 2-sigma or 3-sigma measurements on a typical Kepler light curve allows a magnification threshold of $A_T = 1.001$ or lower to be set (magnification, $A \equiv \text{Flux}/\langle \text{Flux} \rangle$). Since detection is said to occur whenever the magnification $A > A_T$, the effective microlensing tube [15] is wider by a factor of $u_T = [2A_T(A_T^2 - 1)^{-1/2} - 2]^{1/2} \sim 6$.

Here we are using notation [15,16] in which the Einstein ring radius (radius of image ring arising from perfectly aligned source and lens) is $r_E = 0.0193\sqrt{x(1-x)}[(D_s/\text{kpc})m_9]^{1/2}R_\odot$, where $m_9 = (m/10^{-9}M_\odot)$, is the mass of the PBH DM lens, D_s is the source star distance, and $x = D_l/D_s$ is the ratio of the lens distance to source distance. We define the standard microlensing “tube” as that volume along the line-of-sight inside the Einstein ring, and define u to be the transverse distance between the lens and the source center in units of r_E . The important parameter, u_T , is the “effective” radius of the microlensing tube in units of r_E in the point-source limit; thus the usual standard $u_T = 1$ implies $A_T = 1.34$.

The usual point source (PS) optical depth (total number of PBHs inside the microlensing tube), $\tau_{\text{PS}} = \int_0^1 dx D_s \rho(x) \pi u_T^2 r_E^2 / m$, where $\rho(x)$ is the run of DM density along the line-of-sight (LOS), is thus larger than in the standard case by a factor of u_T^2 .

However, just as important for low mass PBH microlensing is the fact that the effective microlensing tube radius is not determined by the Einstein ring radius, but by the radius of the source star due to finite-source effects. For very low mass PBHs, the Einstein ring radius is much smaller than the projected source star radius, xR_* , and u_T in the formula for optical depth should be replaced by u_{thresh} which is the value of the source-lens transverse separation that gives $A = A_T$. The quantity u_{thresh} may be approximated by $u_* = xR_*/r_E$, though below we make a better approximation using the finite-source light curve formulas from Witt & Mao [17]. For $m \approx 10^{-9}M_\odot$ with $x \approx 0.5$ and a typical Kepler source star with $R_* = 1R_\odot$ and $D_s = 1$ kpc, we find $u_* = 51.9$, which gives an optical depth (and total event rate) around 2700 times larger than naively expected. (See below for a more accurate estimate.) Similarly, the usual statement that the optical depth is independent of DM mass is not true in this case. Naively, a lower mass means a narrower microlensing tube, but more DM objects, effects that cancel each other out in the optical depth. For the case where all events are finite-source events, lowering the mass does not change the tube radius, so the optical depth is roughly inversely proportional to mass, increasing the sensitivity to much lower mass DM objects. Likewise, the average event duration, $\langle t_e \rangle$, defined as the time for which the source star is magnified above A_T , is now roughly independent of

mass, and the total event rate, $\Gamma = \tau/\langle t_e \rangle$, now increases roughly inversely with decreasing mass.

Unlike point-source microlensing, there is a limit to the magnification possible from finite-source microlensing:

$A_{\text{max}} = \sqrt{1 + 4/u_*^2}$ [17]. Thus for low mass PBHs, the light curve jumps quickly from near $A = 1$ to $A = A_{\text{max}}$ and then stays roughly constant (actually following the limb-darkening shape of the source star) as the small Einstein ring transits the stellar limb, jumping back to near $A = 1$ at the edge. See Refs. [11,17] for example light curves, which are quite different from standard microlensing light curves. The very precise Kepler photometry is what allows these low magnification finite-source light curves to be detected. For a given A_T , we use the previous equation to find a cutoff, $u_{* \text{max}}$, such that a microlensing event is observable whenever u is less than $u_{* \text{max}} = 2/\sqrt{A_T^2 - 1}$.

The total optical depth and the total event rate include integrals along the LOS, but the limits to these integrals need modification when considering strong finite-source effects. As $x \rightarrow 0$, both the projected source star radius, xR_* , and r_E , go to zero. Their ratio, which is u_* , also goes to zero as $x \rightarrow 0$, while as $x \rightarrow 1$, $r_E \rightarrow 0$ and $u_* \rightarrow \infty$. Because of this last dependence, $A_{\text{max}} \rightarrow 1$ as $x \rightarrow 1$, and so there is always some limiting value of distance, x_{max} , where only objects that enter the tube with $x < x_{\text{max}}$ give detectable magnifications. We find $x_{\text{max}} = 1/(1 + \kappa^2)$, where $\kappa = 51.9(R_*/R_\odot)/(u_{* \text{max}}\sqrt{m_9 D_s/\text{kpc}})$. Thus the optical depth integration limits above should be between $x = 0$ and $x = x_{\text{max}}$, not between 0 and 1.

For the pure finite source case ($u_* \gg u_T$) and a constant DM density, the above optical depth integral can be easily performed. We find $\tau_{\text{FS}} \approx \frac{\pi}{3} D_s \rho R_*^2 x_{\text{max}}^3 / m \approx 4.2 \times 10^{-6} x_{\text{max}}^3 (R_*/R_\odot)^2 (D_s/\text{kpc}) / m_9$. For $A_T = 1.001$, $R_* = 1R_\odot$, $D_s = 1$ kpc, and $m_9 = 1$, we have $x_{\text{max}} = 0.426$ and $\tau_{\text{FS}} = 3.2 \times 10^{-7}$. To estimate the total event rate in this case we can use the very approximate formula from reference [16] or [15], replacing $u_T r_E$ with $x_{\text{max}} R_*$. We find $\Gamma_{\text{pac-FS}} \approx 2\tau_{\text{FS}} v_c / (\pi x_{\text{max}} R_*) = 4.8 \times 10^{-3}$ events/yr/star. The corresponding average event duration is given by $\langle t_e \rangle = \tau/\Gamma \approx 0.59$ h. This is a remarkably large event rate and if 150 000 stars were followed it would result in a total of around 720 detectable events per year.

However, another complication is that for a microlensing event to be detected, it must contain enough significant measurements to be unlikely to occur by chance. For example, given Kepler’s 30 min cadence, monitoring 150 000 stars means about 2.6×10^9 flux measurements per year. Assuming Gaussian errors, the probability of finding 4 sequential measurements 3-sigma above average is such that less than one such instance will occur in 3.5 years of data. This requirement implies an event duration, t_e , the time for which $A > A_T$, of at least 2.0 h. This means that we cannot use the total event rate Γ , but must integrate the differential event rate $\frac{d\Gamma}{dt_e}$ over a relevant range

of event durations. This differential event rate is given in Equation 17 of Ref. [15] for non-finite-source events. In the limit of large u_* this formula can be used just by replacing u_T with u_* throughout. There are also two simplifications to this formula due to the unique position of the Kepler field. First, the Kepler field is at galactic longitude and latitude $(l, b) = (76.32^0, 13.5^0)$ which places it just out of the plane of the Milky Way disk, in almost the same direction in which the solar system is moving [8]. The Kepler source stars, at distances of 1 to 3 kpc, are thus at nearly the same distance from the Milky Way (MW) center as the Sun (8.5 kpc). Thus, unlike the case for the LMC, there is no need to model the halo density and one can just use the local dark matter density $\rho \approx 0.3 \text{ GeV cm}^{-3} = 7.9 \times 10^{-3} M_\odot \text{ pc}^{-3}$ along the entire LOS. Second, since the Kepler stars are in the direction of solar motion and also orbiting the MW center, there is no additional large transverse velocity of the Sun or source to include. Thus Equation 17 of reference[15] becomes

$$\frac{d\Gamma}{dt_e} = \frac{\rho}{m} D_s v_c^2 \int_0^{x_{\max}} dx \beta'^2 g(\beta'), \quad (1)$$

where $g(\beta') = \int_0^1 dy y^{3/2} (1-y)^{-1/2} e^{-\beta' y} = \frac{\pi}{2} e^{-\beta'/2} [I_0(\beta'/2) - (1 + 1/\beta') I_1(\beta'/2)]$, I_0 and I_1 are modified Bessel functions of the first kind, $\beta' = 4r_E^2 u_{\text{thresh}}^2 / (t_e^2 v_c^2)$, $y = v_r^2 / (\beta' v_c^2)$, $v_c \approx 220 \text{ km/s}$, is the halo circular velocity, and we introduced u_{thresh} which stands for u_T in the case of point-source lensing, u_* in the case of pure finite-source lensing, and below will be approximated as something in between for the general case. For use later we note that $g(0) = \frac{3}{8}\pi$, and $g(\beta') \sim \frac{3\sqrt{\pi}}{4} \beta'^{-5/2}$ for large values of β' .

Numerical estimate.—In order to make a reasonably accurate estimate of the potential sensitivity of a search through the Kepler light curve data we need to integrate Eq. (1) from $t_e = t_{\min}$ to some reasonable upper limit. We also want to use realistic distributions of Kepler star distances, radii, and A_T , and we want an approximation for u_{thresh} that interpolates accurately between $u_{\text{thresh}} \approx u_T$ at x near 0, and $u_{\text{thresh}} \approx u_*$ at x near 1. Ideally, we would also include the effects of limb-darkening, but do not do this here. We have done preliminary exploration of this effect by creating limb-darkened finite-source light curves and calculating u_{thresh} for these, and we find this effect usually increases the detection rate by a moderate to small amount depending upon the PBH mass, assumed detection threshold, and stellar parameters.

We looked at a subsample of around 5000 publicly available third quarter Kepler light curves from the NASA MAST website [10]. Besides the light curves of fluxes and flux errors, we have for each star: the stellar radius, R_* , Sloan r and g magnitudes, effective temperature, T_{eff} , star position, extinction parameters A_V

and $E(B - V)$, etc. We estimate the apparent visual magnitude, $V = g - 0.0026 - 0.533(g - r)$ [18], and the stellar distance from $D_s = 1.19 \times 10^{-3} R_*(T_{\text{eff}}/T_\odot)^2 10^{0.2(V - A_V + \text{B.C.})}$ kpc, where B.C. is the bolometric correction. Note that we make a crude bolometric correction, using only the effective temperature and whether the source is a main sequence or giant star [19], but we include it because it slightly reduces the distances to the sources, thereby reducing the expected detection rate, and we want our calculation to be conservative.

To find A_T for each source star, we calculated the average of the reported flux errors over 300 data points near the middle of each light curve, and then estimated each A_T as one plus 3 times this average (for a 3-sigma detection requirement). We also calculated the standard deviation of the flux measurements over this portion of the light curve and found reasonable agreement with the average flux error. For our subsample of 5000 stars we find $2 \times 10^{-5} < A_T - 1 < 3 \times 10^{-3}$, with vast majority having $A_T - 1 \approx 0.001$.

As noted above, the approximation, $u_{\text{thresh}} \approx u_*$ misses some events, since for nearby lenses the projected source radius becomes smaller than the Einstein ring radius, and therefore u_{thresh} should approach u_T rather than zero. To develop a better approximation, we numerically calculated a large set of finite-source light curves using the formula from Witt and Mao [17], and then for each light curve calculated the actual value of u_{thresh} (value of lens-source transverse separation for which $A > A_T$) as a function of u_*/u_T . We find that u_{thresh}/u_T is a fairly universal function of u_*/u_T , and therefore we can calculate u_* for each value of x and find u_{thresh} using this universal function. Our fit function is $u_{\text{thresh}} \approx u_T (1 + .47(u_*/u_T)^2)$, for $u_*/u_T < 0.75$, $u_{\text{thresh}} \approx u_*$, for $u_*/u_T > 4.5$, and $u_{\text{thresh}} \approx u_*/(\sum_i c_i (u_*/u_T)^i)$, with $c_0 = 0.0971$, $c_1 = 0.925$, $c_2 = -0.384$, $c_3 = 0.0723$, and $c_4 = -0.0051$, for $0.75 < u_*/u_T < 4.5$. This approximate u_{thresh} differs from our numerically calculated values by no more than 2.5% over the mass range we investigated.

We then numerically performed the two-dimensional integral of Eq. (1) for various values of PBH mass, various S/N requirements (e.g., four 3-sigma measurements or seven 2-sigma measurements). We summed the total number of expected events over the 5000 stars and then scaled those results to 3.5 years of observation of 150 000 stars, assuming that 25% of these stars will be identified as variable and not be useful [9]. That is we assume 390 000 star-years. Our results are given in Fig. 1. In order to turn these results into the potential sensitivity of detecting PBH dark matter, we calculated the 95% C.L. for each PBH mass, assuming that no events were detected and that there was no background. These potential limits are shown in Fig. 1, along with limits from earlier experiments. The results from the 2 S/N requirements mentioned above were similar so we plot only one.

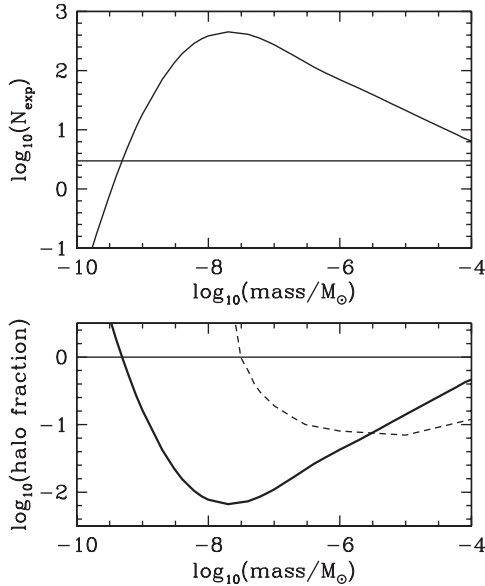


FIG. 1. *Top panel:* The expected number of events, N_{exp} (defined as 4 sequential measurements with flux 3-sigma above average) in 390 000 star-years of Kepler data. The thin horizontal line shows $N_{\text{exp}} = 3$, the limit for a 95% C.L. if no events are detected. *Bottom panel:* Potential 95% C.L. exclusion of PBH dark matter. The area above the thick line would be ruled out if no events were seen in 390 000 star-years. Also shown as a thin dashed line is the limit from combined MACHO/EROS LMC microlensing searches [12]. The thin horizontal line shows a halo consisting entirely of PBHs with local DM density $\rho = 0.3 \text{ GeV cm}^{-3}$.

We see from Fig. 1 that we have the potential to detect or rule out PBHs as the primary constituent of DM over the mass range $5 \times 10^{-10} M_{\odot} < m_{\text{PBH}} < 10^{-4} M_{\odot}$. Current limits from the MACHO/EROS experiments [12] are also shown as a dashed line. There are also limits ruling out halo fractions, $f > 1$, from femtolensing of gamma ray bursts (GRB) [20], but they run from about $10^{-16} M_{\odot} < m_{\text{PBH}} < 10^{-13} M_{\odot}$, off to the left of Fig. 1, and other limits from picolensing of GRBs ruling out $f > 4$ from $4 \times 10^{-13} M_{\odot} < m_{\text{PBH}} < 8 \times 10^{-10} M_{\odot}$, are in our mass range, but too weak to be seen in our plot. We see that a microlensing search for PBHs through Kepler data has the potential to extend the mass sensitivity by almost 2 orders of magnitude below the MACHO/EROS limits which exclude DM masses down to around $2 \times 10^{-8} M_{\odot}$. Note that commonly quoted (e.g., [3]) limits from EROS alone [13] exclude masses down to around $6 \times 10^{-8} M_{\odot}$ and are not as strong as the earlier combined MACHO and EROS limits. There are no other limits in the mass range just below $2 \times 10^{-8} M_{\odot}$, so the capability of Kepler to search for these PBHs is unique.

Discussion and future work.—In this theoretical Letter we suggest a method to detect or rule out PBH DM over a large and unexplored mass range. If nothing is detected the method has the potential to rule out around 40% of the total

remaining mass range for PBH DM. Since microlensing depends only upon lens mass and size, such an experiment would detect or rule out any massive compact halo object dark matter in the mass range described. If PBH DM was discovered this way, the microlensing events would allow excellent characterization of the DM. The finite-source effect and rate dependence on source distance would give information on the mass and velocity distributions, and the nearness of the source stars would make parallax measurements easier than in other microlensing experiments.

We note that this experiment could also detect or rule out ultracompact mini halo DM [21,22], since these would give rise to very similar microlensing signals (see Fig. 3 of [22]).

The next step is clearly to perform the analysis suggested here, and we have begun this task using publicly available Kepler data. This experiment requires deep understanding of the light curve data including instrumental effects. It requires a careful selection of microlensing candidates and an accurate calculation of the efficiency of that selection method, as well as an understanding of false positives and background events. We note that Kepler transit searches have already turned up many stellar flares on M and K dwarfs [23] using selection criteria similar to those used above, and our preliminary search through the data has turned up both asymmetric stellar flare events and microlensinglike candidates. It is clear that a good method of distinguishing microlensing from stellar flares will be needed. If some events are found that are indistinguishable, then the potential limits of Fig. 1 will be weakened by a factor given by Poisson confidence limit statistics [24]; for example, the limits in the lower panel of Fig. 1 should be shifted higher by a factor of 1.6 if one nondistinguishable event is found, by 6.7 if 10 such events are found, etc. However, there are some powerful discriminants against backgrounds. The microlensing light curves should match a limb-darkened finite-source microlensing shape, be non-repeating, and if enough events are found the rates should exhibit the strong dependence on distance and source radius predicted by our formulas.

Our analysis is over simplified and there is much to be done to find actual limits, or, if detected, calculate the PBH contribution to the DM. Our simple 4 contiguous 3-sigma event definition needs to be replaced with selection criteria that do not assume Gaussian noise, and that can reliably remove instrumental effects, variable stars, and flare events. Our treatment of limb-darkening and source star distance needs improvement and the effect of the MW halo model should be considered.

K. G. thanks the IPMU (Tokyo) Focus Week on Dark Matter, where some of the ideas for this paper were started. K. G. and A. M. C. were supported in part by the DoE under grant DE-FG03-97ER40546. A. M. C. was supported in part by the National Science Foundation Graduate Research Fellowship under Grant Number DGE0707423.

B. J. is supported in part by NSF grant AST-0908027 and DOE grant DE-FG02-95ER40893. Some of the data presented in this paper were obtained from the Multimission Archive at the Space Telescope Science Institute (MAST). STScI is operated by the Association of Universities for Research in Astronomy, Inc., under NASA contract NAS5-26555. Support for MAST for non-HST data is provided by the NASA Office of Space Science via grant NNX09AF08G and by other grants and contracts.

-
- [1] S. W. Hawking, *Nature (London)* **248**, 30 (1974).
[2] S. W. Hawking, *Commun. Math. Phys.* **43**, 199 (1975).
[3] B. J. Carr, K. Kazunori, Y. Sendouda, and J. Yokoyama, *Phys. Rev. D* **81**, 104019 (2010).
[4] A. S. Josan, A. M. Green, and K. A. Malik, *Phys. Rev. D* **79**, 3520 (2009).
[5] M. Y. Khlopov, in *Recent Advances on the Physics of Compact Objects and Gravitational Waves*, edited by J. A. de Freitas Pacheco (Research Signpost, Kerala, India, 2007).
[6] P. H. Frampton *et al.*, *J. Cosmol. Astropart. Phys.* **04** (2010) 023.
[7] Borucki *et al.*, *Science* **327**, 977 (2010).
[8] D. Fraquelli and S. E. Thompson, Kepler Archive Manual (KDMC-10008-002) (2011).
[9] <http://kepler.nasa.gov/Science/about/targetFieldOfView>.
[10] <http://archive.stsci.edu/kepler>.
[11] C. Alcock *et al.*, *Astrophys. J.* **471**, 774 (1996).
[12] C. Alcock *et al.*, *Astrophys. J. Lett.* **499**, L9 (1998).
[13] P. Tisserand *et al.*, *Astron. Astrophys.* **469**, 387 (2007).
[14] L. Wyrzykowski *et al.*, arXiv:1106.2925.
[15] K. Griest, *Astrophys. J.* **366**, 412 (1991).
[16] B. Paczynski, *Astrophys. J.* **304**, 1 (1986).
[17] H. J. Witt, and S. Mao, *Astrophys. J.* **430**, 505 (1994).
[18] M. Fukugita *et al.*, *Astron. J.* **111**, 1748 (1996).
[19] B. W. Carroll, and D. A. Ostlie, “*An Introduction to Modern Astrophysics*,” Appendix G (Pearson/Addison Wesley, San Francisco, 2007), 2nd ed.
[20] G. F. Marani *et al.*, *Astrophys. J. Lett.* **512**, L13 (1999).
[21] K. J. Mack, J. P. Ostriker, and M. Ricotti, *Astrophys. J.* **665**, 1277 (2007).
[22] M. Ricotti and A. Gould, *Astrophys. J.* **707**, 979 (2009).
[23] L. M. Walkowicz *et al.*, *Astron. J.* **141**, 50 (2011).
[24] K. Nakamura *et al.* (Particle Data Group), *J. Phys. G* **37**, 075021 (2010).